JGR Atmospheres

RESEARCH ARTICLE
10.1029/2018JD028993

Variations of Lake Ice Phenology on the Tibetan Plateau From 2001 to 2017 Based on MODIS Data

Yu Cai[1,2,3], Chang-Qing Ke[1,2,3,4,5], Xingong Li[6], Guoqing Zhang[7], Zheng Duan[8], and Hoonyol Lee[9]

[1]School of Geography and Ocean Science, Nanjing University, Nanjing, China, [2]Jiangsu Provincial Key Laboratory of Geographic Information Science and Technology, Nanjing University, Nanjing, China, [3]Key Laboratory for Satellite Mapping Technology and Applications of State Administration of Surveying, Mapping and Geoinformation of China, Nanjing University, Nanjing, China, [4]Collaborative Innovation Center of Novel Software Technology and Industrialization, Nanjing, China, [5]University Corporation for Polar Research, Beijing, China, [6]Department of Geography and Atmospheric Science, University of Kansas, Lawrence, Kansas, USA, [7]Chinese Academy of Sciences, Institute of Tibetan Plateau Research, Beijing, China, [8]Chair of Hydrology and River Basin Management, Technical University of Munich, Munich, Germany, [9]Division of Geology and Geophysics, Kangwon National University, Chuncheon, South Korea

Key Points:
- Lakes in the northern Inner Tibetan Plateau (Inner-TP) have longer ice cover durations than those in the southern Inner-TP
- Among 58 lakes, 18 lakes have extending ice cover durations (average 1.11 day/year) and 40 lakes have shortening durations (average 0.80 day/year)
- Lake ice phenology is influenced by climatic conditions, geographical location, and the physico-chemical characteristics of the lakes

Supporting Information:
- Supporting Information S1
- Data Set S1

Correspondence to:
C.-Q. Ke,
kecq@nju.edu.cn

Citation:
Cai, Y., Ke, C.-Q., Li, X., Zhang, G., Duan, Z., & Lee, H. (2019). Variations of lake ice phenology on the Tibetan Plateau from 2001 to 2017 based on MODIS data. *Journal of Geophysical Research: Atmospheres*, *124*, 825–843. https://doi.org/10.1029/2018JD028993

Received 12 MAY 2018
Accepted 21 DEC 2018
Accepted article online 2 JAN 2019
Published online 29 JAN 2019

Abstract Lake ice is a robust indicator of climate change. The availability of information contained in Moderate Resolution Imaging Spectroradiometer daily snow products from 2000 to 2017 could be greatly improved after cloud removal by gap filling. Thresholds based on open water pixel numbers are used to extract the freezeup start and breakup end dates for 58 lakes on the Tibetan Plateau (TP); 18 lakes are also selected to extract the freezeup end and breakup start dates. The lake ice durations are further calculated based on freezeup and breakup dates. Lakes on the TP begin to freezeup in late October and all the lakes start the ice cover period in mid-January of the following year. In late March, some lakes begin to break up, and all the lakes end the ice cover period in early July. Generally, the lakes in the northern Inner-TP have earlier freezeup dates and later breakup dates (i.e., longer ice cover durations) than those in the southern Inner-TP. Over 17 years, the mean ice cover duration of 58 lakes is 157.78 days, 18 (31%) lakes have a mean extending rate of 1.11 day/year, and 40 (69%) lakes have a mean shortening rate of 0.80 day/year. Geographical location and climate conditions determine the spatial heterogeneity of the lake ice phenology, especially the ones of breakup dates, while the physico-chemical characteristics mainly affect the freezeup dates of the lake ice in this study. Ice cover duration is affected by both climatic and lake specific physico-chemical factors, which can reflect the climatic and environmental change for lakes on the TP.

1. Introduction

There are about 1,200 lakes (>1 km^2) on the Tibetan Plateau (TP; Zhang, Yao, Xie, Qin, et al., 2014), and many studies have shown that lake ice phenology (i.e., the timing of freezeup, breakup, and duration of ice cover) responds well to climatic and environmental changes (Brown & Duguay, 2010; Weber et al., 2016). As "the Third Pole of the Earth," the TP is very sensitive to global climate change (Kang et al., 2010; Liu & Chen, 2000; Qiu, 2008). Changes in air and water surface temperatures related to climatic changes are important factors in the lake ice phenology changes (Adrian et al., 2009; Dörnhöfer & Oppelt, 2016; Yao et al., 2016; Zhang, Yao, Xie, Zhang, et al., 2014). At the same time, the state and type of lake ice and their change to open water system in turn affect the local or regional climate (Brown & Duguay, 2010; Rouse et al., 2005). Freezeup/breakup processes can result in sudden changes in lake surface properties (such as albedo and roughness), which affect the water and energy exchange between the lake and the atmosphere (Latifovic & Pouliot, 2007). Therefore, in the context of global climate change, lake ice phenology can be used as a good indicator to monitor the actual impact of climate change on lakes and their surroundings (Ke et al., 2013).

However, due to the harsh environment and limited accessibility, few meteorological stations exist in the central and western TP where lakes are concentrated; thus, it is difficult to carry out field observations. These factors result in a lack of continuous and complete historical records on regional climate changes (Kropáček et al., 2013; Liu & Chen, 2000). Remote sensing data have been widely used in lake ice

monitoring (Duguay et al., 2015; Wei & Ye, 2010). Passive microwave sensors such as the Scanning Multichannel Microwave Radiometer, the Special Sensor Microwave/Image (SSM/I), and the Advanced Microwave Scanning Radiometer for the Earth Observing System (AMSR-E) have high temporal resolutions (at times twice daily or better) and are suitable for monitoring lake ice changes in large lakes, such as Qinghai Lake (Cai et al., 2017; Che et al., 2009) and Nam Co (Ke et al., 2013) on the TP, and Great Bear Lake and Great Slave Lake (Howell et al., 2009) in Canada. However, there are still many medium- and small-size lakes on the TP, which are smaller than the pixel size of passive microwave images (dozens to hundreds of square kilometers). Active microwave sensors have high spatial resolutions (1 m to about 100 m). For example, the European Remote Sensing Satellite (ERS)-1/2 Synthetic Aperture Radar (SAR) has been used for monitoring the lake ice formation process and ice thickness (Duguay & Lafleur, 2003; Jeffries et al., 1994; Morris et al., 1995). Radarsat-1/2 SAR has also been used for monitoring the freezeup/breakup processes of lake ice (Duguay et al., 2002; Geldsetzer et al., 2010). However, the low temporal resolution (for example, three days for ERS and 24 days for Radarsat) of the current active microwave technologies limits the ability to achieve daily monitoring on lake ice (Chaouch et al., 2014; Latifovic & Pouliot, 2007). The medium- and high-resolution optical data, such as Moderate Resolution Imaging Spectroradiometer (MODIS) and Advanced Very High Resolution Radiometer, obtain daily images and are often used to monitor lake freezeup/breakup dates and areas. For example, Weber et al. (2016) used Advanced Very High Resolution Radiometer data to extract the ice phenology of European lakes in different climatic regions. Yao et al. (2016) used MODIS and Landsat data to extract the ice phenology of 22 lakes in the Hoh Xil region of the TP from 2000 to 2011 and analyzed the factors influencing lake ice changes. Chaouch et al. (2014) used MODIS data to monitor the growth and regression of ice in the Susquehanna River in the northeastern United States. However, optical images are obscured by clouds, which limit the direct usage of optical data (Gafurov & Bárdossy, 2009). Currently, there have been many mature cloud removal methods, including methods based on temporal and spatial continuity (Gafurov & Bárdossy, 2009; López-Burgos et al., 2013; Paudel & Andersen, 2011) and methods combining multiple sensor data (Gao, Xie, Lu, et al., 2010; Gao, Xie, Yao, et al., 2010; Liang et al., 2008), which can reduce cloud cover and increase data availability by gap filling approaches and/or compositing.

The unique geographical and climatic conditions of the TP make it a region of high interest for climate research (Kang et al., 2010). Owing to the low annual air temperature, many lakes on the TP have long and stable ice cover periods during winter. Recent studies on individual lakes have shown that on the TP, the freezeup dates of some lakes have been delayed, the breakup dates have advanced, and the ice cover durations have significantly shortened (Cai et al., 2017; Che et al., 2009; Ke et al., 2013). However, there are few ice phenology studies covering the entire TP. Guo et al. (2018) used MODIS reflectance data, eight-day synthetic snow product, and land surface temperature data to analyze the uncertainty and variation of different remotely sensed lake ice phenology across the TP. Kropáček et al. (2013) used MODIS eight-day synthetic snow products to analyze the ice phenology changes of 59 large lakes on the TP from 2001 to 2010. However, the eight-day interval could not capture the lake ice phenology very precisely, especially for the start and end dates of freezeup and breakup. To date, to our best knowledge, no existing study has used MODIS daily snow products to study the lake ice phenology on the TP.

To obtain the lake ice phenology variations on the TP, the daily snow products of MODIS are used to extract the freezeup and breakup dates of lake-wide ice cover from 2001 to 2017. The lake ice durations are then calculated, and the spatial variabilities and change rates of lake ice phenology are analyzed. Using reanalysis data and available satellite data set, the effects of air temperature, lake surface water temperature, and wind speed on lake ice phenology are analyzed. In addition, possible influence of geographical determined lake locations and physico-chemical conditions on lake ice phenology are also investigated.

2. Study Area

The TP is located in central Asia; it is the largest plateau in China, and its elevation is the highest in the world. The TP is known as the "roof of the world" and the Third Pole of the Earth, with an average elevation of over 4,000 m above sea level and a total area of approximately 3.0×10^6 km^2 (Qiu, 2008; Zhang et al., 2013). There are about 1,200 lakes (>1 km^2) on the TP with a total size of 47,000 km^2, which accounts for more than 50% of the total size of Chinese lakes (Zhang, Yao, Xie, Qin, et al., 2014), in which 389 lakes have an area

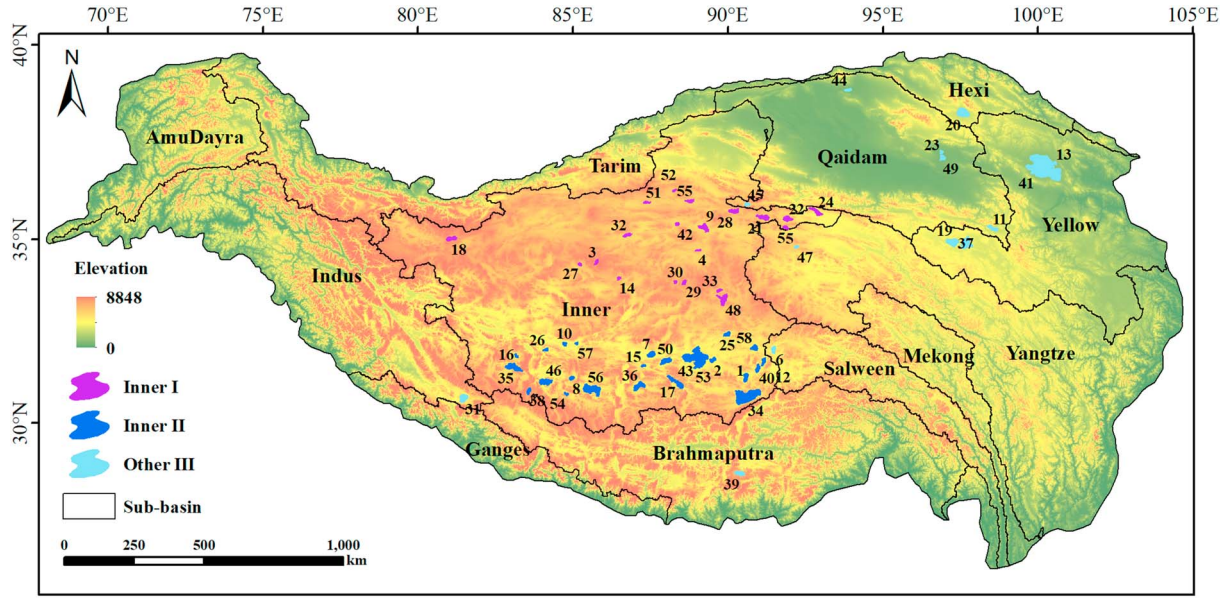

Figure 1. Locations of the TP and its subbasins. Fifty-eight study lakes are grouped into three subareas labeled inner I, inner II, and other III (the lake names are listed in Table A1 in Appendix A).

larger than 10 km^2, including three lakes larger than 1,000 km^2: Qinghai Lake (4,254.90 km^2), Selin Co (2,129.02 km^2), and Nam Co (2,040.90 km^2; Wan et al., 2014).

By analyzing the freezeup/breakup characteristics for each lake on the TP, 58 lakes with a stable ice cover period (less cloud cover, less pixel misclassification, and obvious ice cover period) are manually selected as study lakes (Figure 1), including three lakes larger than 1,000 km^2, 35 lakes larger than 100 km^2, and 20 lakes smaller than 100 km^2, in which the smallest lake is Xuemei Lake (41.33 km^2; Wan et al., 2014). Most lakes (>70%) are in the Inner basin (Zhang et al., 2013). To analyze the spatial variability of lake ice phenology, the Inner basin is divided into upper and lower parts (Inner I and Inner II, northern and southern parts separated around the latitude of 33°N; Zhang et al., 2013), and lakes outside the Inner basin are classified as Other III (Figure 1). The lake boundaries used were extracted from Landsat images (Wan et al., 2014), and all data sets involved in the extraction and comparisons are clipped by the same lake boundary. An annual period extends from 1 August to 31 July of the following year; for example, 1 August 2012 to 31 July 2013 is noted as the annual period of 2013.

3. Data and Methods

3.1. Data

3.1.1. MODIS Daily Snow Cover Products

MODIS is mounted on the Terra and Aqua satellites, which obtain global observation data every one or two days. The available daily snow cover products with a spatial resolution of 500 m from MODIS include MOD10A1 (Terra) and MYD10A1 (Aqua). The available temporal range of MOD10A1 is from 1 August 2000 to 31 July 2017 and that of MYD10A1 is from 1 August 2002 to 31 July 2017. Four MODIS tiles (h24v05, h25v05, h25v06, and h26v05) cover the 58 lakes of this study. The data were obtained from the U.S. National Snow and Ice Data Center (http://nsidc.org/; version 5 for 2001–2016 and version 6 for 2017) on 8 September 2017.

The accuracy of the daily snow cover products of MODIS are approximately 93% under clear-sky conditions (Hall & Riggs, 2007; Huang et al., 2011; Maurer et al., 2003; Parajka & Blöschl, 2008; Sorman et al., 2007). However, the daily snow cover products over the TP have a yearly average cloud cover (>40%) from MODIS observations (Yu et al., 2016), and need to be processed for cloud removal by gap filling. Some lakes may have snow covering the ice surface during the ice cover period, and MODIS snow cover products could classify these ice-covered pixels into snow-covered pixels, which results in a low lake ice cover compared to

the lake size (Kropáček et al., 2013). Therefore, the changes of lake water cover proportions (the proportion of the lake covered by open water) are used to extract the freezeup/breakup dates, and the lake ice cover proportions are used to assist in correcting the date results. Under clear-sky conditions, the reduction in water cover is considered as the result of lake ice cover increase.

3.1.2. Landsat Data

The Landsat program is a series of Earth observing satellites, which is comanaged by the National Aeronautics and Space Administration and the United States Geological Survey to monitor Earth and environmental resources. Since 23 July 1972, eight satellites have been launched including Landsat Multispectral Scanner (MSS; ~80 m) and Thematic Mapper (TM; 30 m)/Enhanced Thematic Mapper Plus (ETM+; 30 m)/Operational Land Imager (OLI; 30 m) with a temporal resolution of 16 days. Landsat data used are from the standard United States Geological Survey Landsat Surface Reflectance products (Collection 1 Level-2) of Landsat 5, 7, and 8 from 2000 to 2017 on the Google Earth Engine platform (https://earthengine.google.com/). Images without cloud cover and obtained during the freezeup or breakup periods are selected to extract the lake water cover proportions.

To extract lake ice, pixels covering a lake need to be first distinguished from other types of pixels, such as cloud and land. A threshold of 0.4 for Normalized Difference Snow Index (NDSI; Hall et al., 2001) is applied to extract the extent of a lake as follows:

$$\mathrm{NDSI} = (\mathrm{TM\ Band\ 2} - \mathrm{TM\ Band\ 5})/(\mathrm{TM\ Band\ 2} + \mathrm{TM\ Band\ 5}) \geq 0.4 \quad (1)$$

Then, according to the actual reflectance of each image, different thresholds on the near-infrared band are set to distinguish lake ice from lake water. Finally, the proportion of lake water within a lake boundary (1 − ice cover proportion) is calculated and compared with MODIS results on the same day to verify the accuracy of using MODIS snow cover products after cloud removal by gap filling.

3.1.3. Lake Ice Phenology Products From AMSR-E/2 Data

The daily lake ice phenology time series derived from AMSR-E and AMSR2 by Du et al. (2017) provide 5-km ice phenology retrievals describing daily lake ice conditions over the Northern Hemisphere (http://files.ntsg.umt.edu/data/AMSRE2_LAKE_ICE_PHEN/). The data set is used for lake-wide comparisons with MODIS data results from 2003 to 2011 and from 2013 to 2015. Pixels within the lake boundary are extracted for eight lakes larger than 500 km^2. Considering the differences between passive microwave and optical data and the difference in data productions, when the number of ice-on pixels account for more than 10% of all pixels in the lake, the date is determined to be freezeup start date, and less than 10% is breakup end date.

3.1.4. Reanalysis Meteorological Data

The National Centers for Environmental Prediction/National Center for Atmospheric Research reanalysis data set is a joint product from the National Centers for Environment Prediction and the National Center for Atmospheric Research (https://www.esrl.noaa.gov/). This data set provides reanalysis meteorological data every 6 hr including air temperature, air pressure, relative humidity, and wind speed at a spatial resolution of 2.5° from 1 January 1948 to present. The monthly mean data of near-surface air temperature and wind speed are used.

To match the annual ice period, the annual mean air temperature and wind speed are calculated from August of the current year to July of the following year. Then, the change rates of air temperature and wind speed from 2001 to 2017 are calculated. Finally, the inverse distance weighted method is used to interpolate and calculate the means and change rates of air temperature and wind speed for each lake over the 17 years.

3.2. Methods

3.2.1. Cloud Removal for the MODIS Snow Product

The cloud removal (gap filling) process has two steps. The first step is to combine daily Terra and Aqua snow cover products to determine lake cover type (Gafurov & Bárdossy, 2009). For a pixel A, if any of the pixels on Terra or Aqua images for the same day is open water (or other useful pixel types such as ice and snow, the same below), the pixel on the output image is determined to be covered by water. When the pixel is covered with clouds (or other useless types such as land and missing data, the same below) on both Terra and Aqua images, the output pixel is determined to be cloud covered (Gafurov & Bárdossy, 2009):

$$S_{(A,\text{output})} = \text{water if } S_{(A,\text{Aqua})} = \text{water OR } S_{(A,\text{Terra})} = \text{water} \quad (2)$$

$$S_{(A,\text{output})} = \text{cloud if } S_{(A,\text{Aqua})} = \text{cloud AND } S_{(A,\text{Terra})} = \text{cloud} \quad (3)$$

Since Aqua satellite was launched in 2002, there is no first step data process for the 2001–2002 period. The images from step one are used as the inputs for the following step. The second step is based on the temporal correlation of cloud cover pixels (Gafurov & Bárdossy, 2009). First, if a pixel A on date t is cloud covered, the pixels on the images of previous and next days will be searched, and if both pixels are covered by water, pixel on date t is determined to be covered by water as follows (Gafurov & Bárdossy, 2009):

$$S_{(A,t)} = \text{water if } S_{(A,t-1)} = \text{water AND } S_{(A,t+1)} = \text{water} \quad (4)$$

If pixel A on date $t-1$ is cloud covered, then the pixel on date $t-2$ will be searched, and if both pixels on date $t-2$ and date $t+1$ are water covered, the pixels on date t and $t-1$ will be replaced by water. Similarly, if the pixel on date $t+1$ is cloud covered, the pixel on date $t+2$ will be searched as follows (Gafurov & Bárdossy, 2009):

$$S_{(A,t-1)}, S_{(A,t)} = \text{water if } S_{(A,t-2)} = \text{water AND } S_{(A,t+1)} = \text{water} \quad (5)$$

$$S_{(A,t)}, S_{(A,t+1)} = \text{water if } S_{(A,t-1)} = \text{water AND } S_{(A,t+2)} = \text{water} \quad (6)$$

3.2.2. Extraction of Freezeup/Breakup Dates

Often, there will be an unfrozen area near a lake's outlet during the freezeup period, and a small amount of accumulated lake ice on the lakeshore during the breakup process (Reed et al., 2009; Yao et al., 2016). In addition, repeated freezeup and breakup periods caused by weather changes, mismatch of lake boundaries, misclassification of pixels, and inevitable noise (especially cloud cover) will change the extraction of lake ice phenology. Therefore, Kropáček et al. (2013) proposed using 5 and 95% of the lake area as thresholds to extract ice phenology instead of 0 and 100%. Furthermore, images with a cloud cover of more than 50% over a lake after gap filling are eliminated to reduce the influence from sudden changes in water cover.

First, a median M of all the lake water cover proportions in a year is calculated. Then, all the water cover proportions are divided into two groups: one group (G_h) contains the values greater than M and the other group (G_l) contains the values less than M, and the mean values of both groups are calculated. Two thresholds are determined by using the 5 and 95% of the two mean values as follows (Kropáček et al., 2013):

$$Th_h = 95\%M_h + 5\%M_l \quad (7)$$

$$Th_l = 5\%M_h + 95\%M_l \quad (8)$$

where M_h and M_l are the mean values of group G_h and G_l, respectively. Since the freezeup/breakup processes of lakes are usually short, M_h can represent the typical proportion of a lake covered by water during the non-ice cover period, and M_l can represent the typical water cover proportion during ice cover period (Kropáček et al., 2013). The dates when the water cover no longer raises above the thresholds (Th_h for freezeup start date and Th_l for freezeup end date) again during the freezeup period and no longer drops below the thresholds (Th_l for breakup start date and Th_h for breakup end date) during the breakup period are extracted as lake ice phenology dates. Sometimes the remnant cloud cover (or other useless pixels) will decrease the water cover, making it smaller than the thresholds. Therefore, after automatic extraction, the extracted dates need to be checked again by visual interpretation on the water, ice, and cloud cover changes within a year (Figure 2).

The four freezeup/breakup dates divide the annual status of lake ice into four periods and the corresponding durations can be calculated: freezeup duration (FUD; from freezeup start to freezeup end), breakup duration (BUD; from breakup start to breakup end), complete freezing duration (CFD; from freezeup end to breakup start), and ice cover duration (ICD; from freezeup start to breakup end).

3.2.3. Statistical Analysis

The mean absolute error (MAE), correction of determination (R^2), and bias are measured for comparisons between the MODIS cloud-removed and Landsat data as well as comparisons between ice phenology results derived from MODIS and passive microwave data sets. Trend significances of lake ice dates and durations

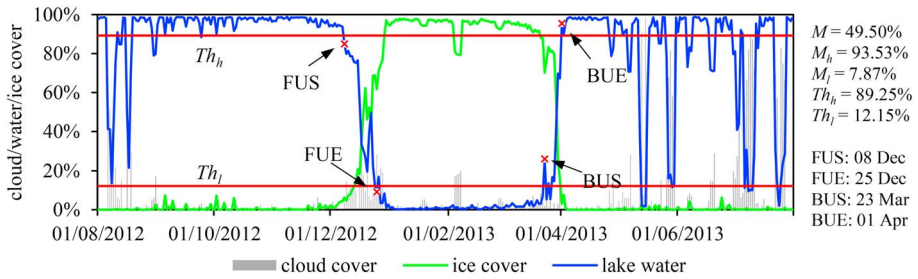

Figure 2. The extraction of the freezeup/breakup dates in Qinghai Lake during 2013. Two red lines represent the two thresholds for extracting freezeup/breakup dates, and four red stars, from left to right, represent the freezeup start (FUS), freezeup end (FUE), breakup start (BUS), and breakup end (BUE) dates.

are evaluated using the nonparametric Mann-Kendall test (Kendall, 1975; Mann, 1945). Furthermore, the relationships between lake ice phenology parameters and climate conditions are evaluated using the coefficient of correlation (r).

4. Results

4.1. Cloud Removal of MODIS Snow Cover Products and Validation Using Landsat Data

4.1.1. Cloud Removal by Gap Filling

Taking the year 2013 as an example, before gap filling, the mean cloud cover of the 58 lakes is 44.97 and 51.70% for Terra and Aqua, respectively. After the first step of combining the data from two satellites, the cloud cover is eliminated to 31.02%. After the second step of using pixels in neighboring dates, the mean cloud cover is eliminated to 16.54%. Taiyang Lake has a mean cloud cover of more than 60%, which is the highest among 58 lakes, and it is eliminated to 35.49% after the cloud removal. For some lakes, the cloud cover can even be eliminated to less than 5% after cloud removal (Table 1). For example, the mean cloud cover of Qinghai Lake in 2013 after cloud removal is 7.54%, and the freezeup/breakup dates can be clearly distinguished (Figure 2).

4.1.2. Validation

For some large lakes, such as Qinghai Lake, Landsat images cannot cover the entire lake on the same day and images acquired from different days cannot be mosaicked to extract the lake ice. Often, the freezeup/breakup period of a lake is only a dozen of days, which is usually not captured by Landsat images due to the 16-day temporal resolution. In addition, considering the influence of cloud cover, there are indeed few available Landsat images. Therefore, lakes which can be covered by one Landsat image and those with relatively long freezeup/breakup period are preferably selected for validation.

A total of 28 Landsat images covering Nam Co (19 images) and Selin Co (9 images) during the freezeup or breakup periods are selected. The proportions of lake water to total lake area are calculated for each image and compared with the water cover proportions from the cloud removed MODIS data. The R^2 is 0.95, the mean absolute error (MAE) is 4.58%, and the bias is 2.09% (Figure 3), indicating a relatively high accuracy, and MODIS data can be used to detect lake water changes well after cloud removal by gap filling.

4.2. Comparisons With Other Lake Ice Data Sets

Daily passive microwave brightness temperature data, including AMSR-E/2 and SSM/I, are used for cross-validation with MODIS lake ice phenology results. The freezeup start and breakup end dates of eight lakes (larger than 500 km^2) derived from AMSR-E/2 pixel-size lake ice phenology products (Du et al., 2017) from 2003 to 2015 (except 2012) are compared with MODIS data with results are shown in Table 2. The breakup

Table 1
Comparison of Cloud Cover for 58 Lakes During 2013, With and Without Cloud Removal

	Mean	Maximum	Minimum
Original Terra	44.97%	63.98% (Taiyang Lake)	30.07% (Zhaxi Co)
Original Aqua	51.70%	69.43% (Taiyang Lake)	31.47% (Mapam Yumco)
Combined T&A	31.02%	50.94% (Taiyang Lake)	18.58% (Lagkor Co)
Cloud removal	16.54%	35.49% (Taiyang Lake)	4.52% (Zhari Namco)

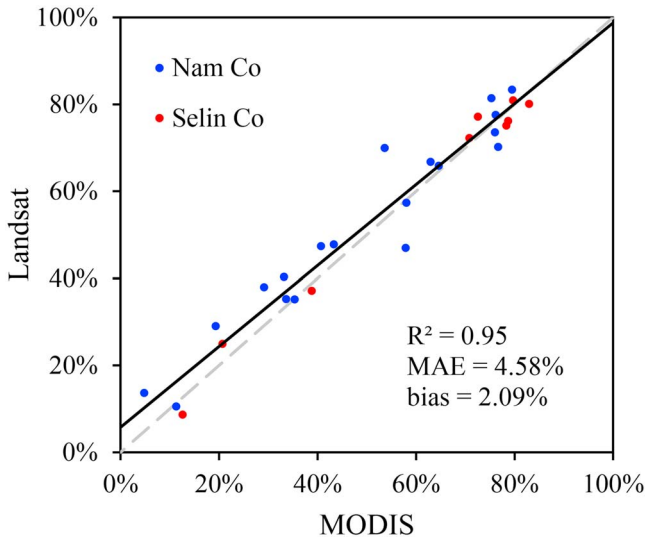

Figure 3. Comparison of lake water cover proportions during freezeup/breakup periods derived from the MODIS cloud-removed data and Landsat data.

end dates from two data sets are strongly correlated (average $R^2 = 0.90$) but the freezeup start dates have relatively low consistency (average $R^2 = 0.35$). Generally, MODIS dates are earlier than AMSR dates, but vary from lake to lake (Table 2). The MAEs of freezeup start dates range for eight lakes from 2.92 to 7.25 days and breakup end dates range from 1.75 to 3.25 days.

Furthermore, ice phenology data for Qinghai Lake from 2001 to 2016 (Cai et al., 2017) and Nam Co from 2001 to 2013 (Ke et al., 2013) derived from SSM/I data are also compared with MODIS results. The correlations of freezeup start and breakup end dates for Nam Co are low ($R^2 = 0.42$ and 0.35, respectively) and the MAEs are both over six days (Table 2). The freezeup start date from MODIS data is obviously earlier than SSM/I data (bias = −5.28 days), probably because Nam Co is covered by merely one SSM/I pixel and less information can be provided. On the other hand, Qinghai Lake provided four freezeup/breakup dates for comparison with MODIS data. Similar to AMSR results, the consistency of freezeup dates are lower than breakup dates (Figure 4). Moreover, in Qinghai Lake, freezeup dates from MODIS data are earlier than passive microwave data (both SSM/I and AMSR) while breakup dates are later (Figure 4), which could be attributed to coarser spatial resolution of passive microwave images and absence of ice information along the lakeshore (Cai et al., 2017). The MAE of freezeup end date is the largest (6.56 days) and the MAEs of breakup dates are about two days (Figure 4). These results indicate that the influence from different remote sensing data and different data production processes on freezeup dates may be larger than that on breakup dates. It is similar to the results of Du et al. (2017) when they compared AMSR lake ice phenology results with Canadian Ice Service and IMS data. Since many lakes start to freezeup near the lakeshores, passive microwave data may ignore the initial ice formation (Cai et al., 2017). In addition, thin ice may be undetectable by the defined brightness temperature thresholds (Du et al., 2017). Furthermore, during the freezeup period, cloud cover from frequent rain and snow weather may increase the uncertainty of the freezeup dates extraction from MODIS data. These factors may cause the low correlations between passive microwave and MODIS derived freezeup start dates.

4.3. Ice Phenology and Its Change of the Lakes on the TP From 2001 to 2017

For each of 58 lakes, freezeup start and breakup end dates are extracted, and their corresponding ice cover durations are calculated. Some lakes do not freezeup completely in winter due to mild winters, large water volume, and/or high salinity (Kropáček et al., 2013), and some lakes are obscured by cloud and/or misclassified pixels during ice cover period. Apart from these lakes, for 18 lakes with characteristic

Table 2
Summary of the Comparison Results for Freezeup Start (FUS) and Breakup End (BUE) Dates Derived From MODIS Snow Products, AMSR-E/2 Data Sets, and SSM/I Data Sets

		FUS			BUE		
	Lake Name	R^2	Bias	MAE	R^2	Bias	MAE
MODIS compared with AMSR-E/2	Gyaring Lake	0.09	0.50	5.33	0.97	0.67	2.50
	Har Lake	0.62	−0.58	2.92	0.84	−0.83	2.17
	Nam Co	0.19	3.58	7.08	0.79	0.75	3.25
	Ngangla Ringco	0.28	−4.33	5.83	0.91	−0.17	1.83
	Ngoring Lake	0.19	0.83	6.83	0.93	−0.58	2.25
	Qinghai Lake	0.41	2.25	3.42	0.86	−0.75	2.25
	Selin Co	0.48	−7.25	7.25	0.93	0.75	1.75
	Zhari Namco	0.54	−2.83	3.83	0.96	−1.50	2.00
	Average	0.35	−0.98	5.31	0.90	−0.21	2.25
MODIS compared with SSM/I	Nam Co	0.42	−5.38	6.92	0.35	0.00	6.31
	Qinghai Lake	0.32	0.44	4.69	0.85	−1.56	2.56
	Average	0.37	−2.47	5.81	0.60	−0.78	4.44

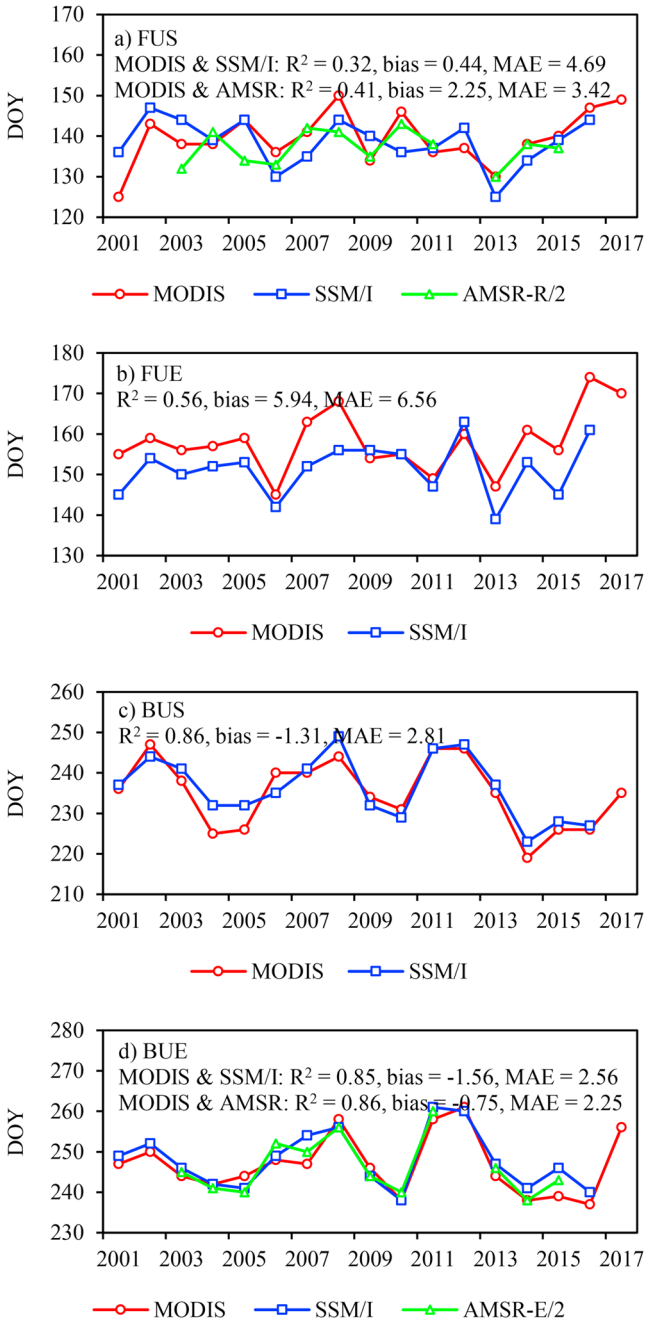

Figure 4. Comparisons of ice phenology for Qinghai Lake derived from MODIS data and passive microwave data. (a) Comparisons between freezeup start (FUS) dates derived from MODIS, SSM/I, and AMSR. (b) Comparisons between freezeup end (FUE) dates derived from MODIS and SSM/I. (c) Comparisons between breakup start (BUS) dates derived from MODIS and SSM/I. (d) Comparisons between breakup end (BUE) dates derived from MODIS, SSM/I, and AMSR. DOY means the day of the year relative to 1 August.

change of water cover proportions, the freezeup end and breakup start dates are also extracted, and four lake ice durations (i.e., freezeup duration, breakup duration, complete freezing duration, and ice cover duration) are calculated, such as Har Lake in Figure 5. Based on the four freezeup/breakup dates and four durations from 2001 to 2017, their mean values and change rates of ice phenology for the 58 lakes are shown in Appendix Table A1. Additional statistics are shown in Appendix Table A2 and Table 3.

4.3.1. Freezeup/Breakup Dates

Around late October, Yuye Lake has begun to freeze up, which is the earliest among 58 lakes. After Taro Co had begun to freeze up by mid-January of the following year, all the lakes on the TP have started their ice cover periods. The gap between freezeup start dates among the lakes can be as long as 90.47 days. From late March to early July, the lakes have ended their ice period one after another, and the earliest and latest lakes are Tuosu Lake and Gozha Co, respectively. Generally, the spatial differences in the freezeup dates are smaller than the breakup dates (Table A2). The mean freezeup start date for the lakes in the Inner I is 32.68 days earlier than that of the lakes in the Inner II, while the mean breakup end date in the Inner I is 43.56 days later than that in the Inner II (Figure 6 and Table 3).

Freezeup/breakup dates for many lakes on the TP have obvious change tendencies from 2001 to 2017 (Table A1). For example, the freezeup start and freezeup end dates for Har Lake have been delayed at a rate of 0.66 and 0.35 day/year, respectively, and the breakup start and breakup end dates have advanced at rates of 0.38 and 0.12 day/year, respectively (Figure 5). Overall, the change rates of freezeup dates for most lakes are more significant than the breakup dates (Table A1). Except for a few lakes in the eastern Inner I which have advancing trends in the freezeup dates, 47 lakes (81.03%) show delayed trends from 2001 to 2017. All the lakes in the Inner II have delayed trends during the 17 years (Figure 6b and Table 3). Among the 58 lakes, the lakes with delayed and advancing trends of breakup dates are both 50% (Table 3). Spatially, the delayed trend is more pronounced than the advancing trend (Figure 6d). Lakes in the Inner I, such as Dogaicoring Qangco and Lexiewudan Co (change rates of the breakup end dates are 3.50 and 4.25 day/year, respectively; Table A1), experienced the most dramatic changes (Figure 6d). During the 17 years, 35 lakes show an opposite change trend of freezeup and breakup dates, and another 21 lakes show the same delayed change trend. Only Huolunuo'er and Meiriqiecuomari have the same advancing trend of freezeup and breakup dates (Table A1).

4.3.2. Lake Ice Durations

Lake ice cover durations on the TP differ greatly, where the duration of the shortest lake (Taro Co) is 86.59 days, and that of the longest lake (Xuemei Lake) is approximately 240.94 days (Table A2). The spatial distribution of the ice cover duration is consistent with that of the freezeup/breakup dates: the lakes in the Inner II with later freezeup and earlier breakup have shorter ice cover durations, and the lakes in the Inner I with earlier freezeup and later breakup have longer ice cover durations (Figure 7a), which is 76.25 days longer on average than those of the Inner II (Table 3). Among the 18 lakes extracted complete four freezeup/breakup dates, 13 lakes (72.22%) have shorter freezeup durations than breakup durations; that is, freezeup takes place faster than breakup does (Table A1). However, the variations in freezeup durations

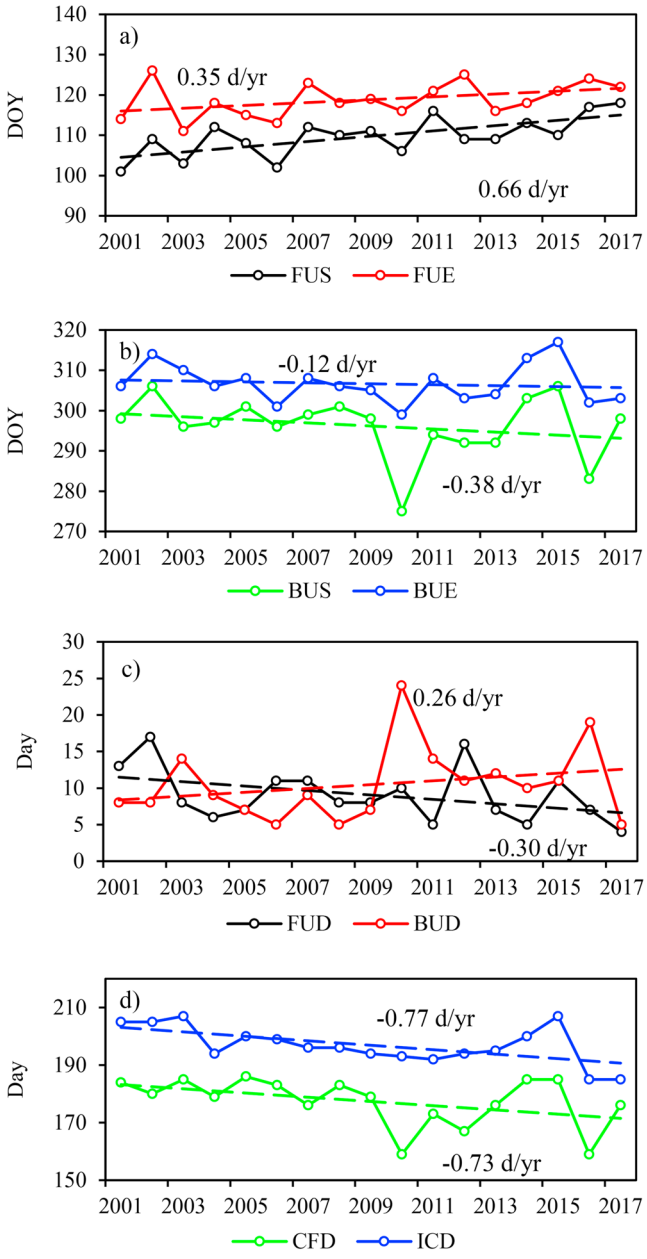

Figure 5. The ice phenology and its trend for Har Lake from 2001 to 2017. (a) Freezeup dates and their trends. (b) Breakup dates and their trends. (c) Freezeup duration and breakup duration and their trends. (d) Complete freezing durations and ice cover duration and their trends over 17 years. FUS: freezeup start, FUE: freezeup end, BUS: breakup start, BUE: breakup end, FUD: freezeup duration, BUD: breakup duration, CFD: complete freezing duration, and ICD: ice cover duration.

among the lakes are larger than that in breakup durations (Table A2). Among the 18 lakes, Hoh Xil Lake has the earliest freezeup end date and the latest breakup start date; thus, the longest complete freezing duration is up to 209.65 days. Qinghai Lake has the shortest complete freezing duration of 76.82 days (Table A2).

Over the 17 years, 40 lakes (68.97%) display a shortening trend in ice cover duration. For example, Har Lake has a shortening trend of 0.77 day/year (Figure 5d). Lakes with extending trends are mainly concentrated in the eastern part of the Inner I (Figure 7b). Since all the lakes in the Inner II have delayed trends of freezeup start dates, 21 lakes (87.50%) have their ice cover durations shortened. Similar to freezeup/breakup dates, half of the lakes in the Inner I have shortening ice cover durations and the other half have extending durations (Table 3). The trends of complete freezing duration for the 18 lakes are mainly consistent with the trends of ice cover duration. Lakes such as Hoh Xil Lake and Tu Co have a shortening freezeup and breakup durations, despite an extending ice cover duration. Although lakes such as Dagze Co and Ngangze Co have shortening trends of ice cover duration, their shortening freezeup and breakup duration results in an extending trend of complete freezing duration. Of the lakes, 77.78% show the same trend in freezeup and breakup durations (Table A1). There are several lakes, such as Har Lake, which have shortening freezeup durations and extending breakup durations (Figure 5c). The freezeup and breakup durations of most lakes (both 72.22%) have shortened over 17 years, which indicates that freezeup/breakup takes place faster (Table A1).

5. Discussions

5.1. Uncertainty Analysis

Errors in the extraction of the ice phenology from MODIS snow cover products mainly come from three aspects: (1) the MODIS snow cover products have cloud cover, misclassification, and occasional missing data; (2) changes to the original data caused by cloud removal; and (3) misjudgment when extracting the lake ice phenology dates. While the quality of MODIS snow cover products cannot be changed, the proportion of usable pixels can be increased by removing some of the cloud cover by gap filling. Combining Terra and Aqua data can solve the problem of missing dates, and combined with the temporal information of cloud (noise) covered pixels, about two thirds of the cloud and other noise pixels can be eliminated. Cloud cover could reflect most of the solar radiation, so the cloud cover in a short period of time would not have much impact on lake surface coverage (Gafurov & Bárdossy, 2009). Possible increased lake ice caused by snowfall during cloudy days (or low temperature at night) is ignored if they break up on the following sunny day (or in the daytime). According to the study of Gafurov and Bárdossy (2009), the performance accuracy of the gap-filling approach is more than 95%. To maintain with the original MODIS information as much as possible, the cloud-removal process only considers the temporal information one to two days before and after the present day, and the potential error can be controlled within two days. Although the possible error in the gap-filling process is minimized, the remaining and persistent (longer than two days) cloud cover will still influence the extraction of ice phenology dates.

Table 3
The Number and Percentage of Lakes, Their Mean Date/Days, and Change Rates (day/year) Within Three Subareas: Inner I, Inner II, and Other III (FUS: Freezeup Start, BUE: Breakup End, and ICD: Ice Cover Duration)

		Inner I	Inner II	Other III	All Lakes
FUS	Mean (all)	20 (34.48%), 10 November	24 (41.38%), 13 December	14 (24.14%), 5 December	58 (100%), 30 November
	Delaying	10 (50.00%), 0.57	24 (100.00%), 0.64	13 (92.86%), 0.35	47 (81.03%), 0.55
	Advancing	10 (50.00%), −0.49	0	1 (7.14%), −0.00	11 (18.97%), −0.44
BUE	Mean (all)	3 June	20 April	26 April	6 May
	Delaying	12 (60.00%), 1.21	11 (45.83%), 0.32	6 (42.86%), 0.35	29 (50.00%), 0.69
	Advancing	8 (40.00%), −0.51	13 (54.17%), −0.44	8 (57.14%), −0.19	29 (50.00%), −0.39
ICD	Mean (all)	204.46	128.21	141.79	157.78
	Extending	11 (55.00%), 1.62	3 (12.50%), 0.41	4 (28.57%), 0.24	18 (31.03%), 1.11
	Shortening	9 (45.00%), −0.92	21 (87.50%), −0.89	10 (71.43%), −0.50	40 (68.97%), −0.80

The remaining cloud cover (or other useless pixels) will decrease the lake water/ice cover of the day, and sometimes the automatic extraction method may obtain a wrong date. However, these mistakes can be modified by later manual correction of comparing the water/ice/cloud curves of that year. Using thresholds can control the difficulty caused by repeated freezeup and breakup of lake ice and ensure the consistency of the freezeup/breakup date extractions. For example, there were several periods of repeated freezeup and breakup at the start of the breakup process in Qinghai Lake in 2013. It is difficult to determine which breakup date should be extracted without using a threshold. Although the extracted date seems like a noise date, the ice cover has definitely dropped after that day, so the date is determined to be the breakup date of that year (Figure 2). Although some dates will be checked and modified after automatic extraction, the initial dates are all selected based on the thresholds. Considering the existence of noise, the thresholds are set to 5 and 95% instead of the extreme values. This approach may cause the later extraction of the freezeup start and breakup start dates, and earlier of the freezeup end and breakup end dates. But without available validation data, the actual error cannot be accurately evaluated. However, the same rule is applied to all the lakes and in all the years, which makes possible the comparisons between lakes and years.

The persistent cloud cover is difficult to be eliminated. But similarly, without surface observation data, the errors cannot be accurately evaluated. It seems that some lakes have the feature that cloud covered most areas during freezeup and/or breakup periods. However, lakes with too much noise or complex shape (for

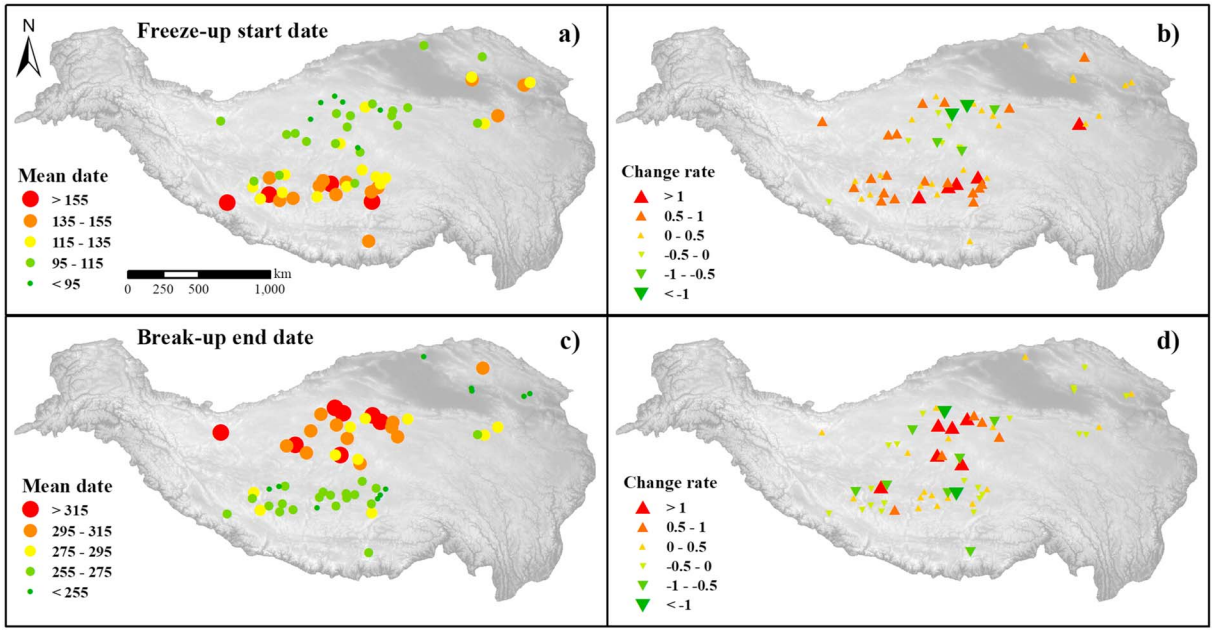

Figure 6. Mean and change rate (day/year) of freezeup start and breakup end dates of the 58 lakes from 2001 to 2017. (a) Mean freezeup start date. (b) Change rate of freezeup start date. (c) The mean breakup end date. (d) Change rate of breakup end date. The freezeup/breakup dates are DOYs.

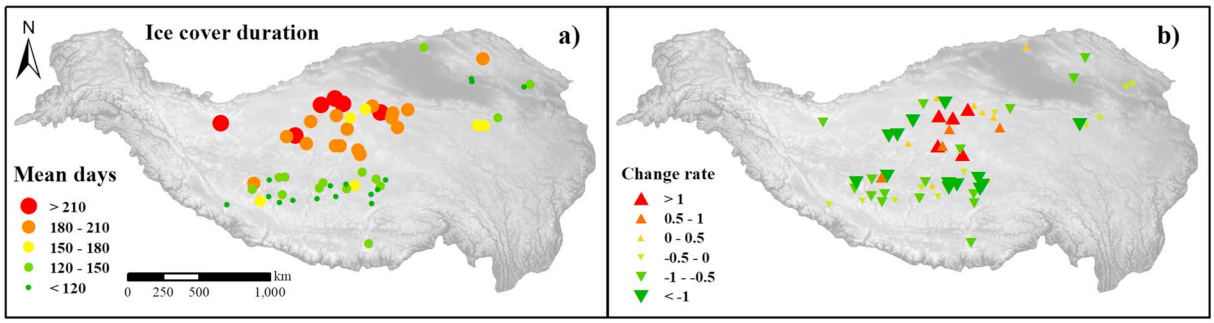

Figure 7. Mean and change rate of ice cover duration for the 58 lakes from 2001 to 2017. (a) Mean ice cover duration. (b) Change rate of ice cover duration.

example, Bangong Co is long and narrow and Yamzho Yumco is tentacle-like) that cannot guarantee the reasonable dates have already been excluded in the lake selection period. Furthermore, some lakes have persistent cloud cover after they begin to freezeup, which is probably caused by misclassification of ice to cloud. If the cloud cover influences the extraction of the freezeup end and/or breakup start date, the dates will not be extracted. Only lakes with clear curves of water/ice changes are chosen in order to obtain more accurate dates, even if the cost is that the number of the selected lakes will be reduced.

Kropáček et al. (2013) extracted the lake ice phenology of 59 large lakes on the TP from 2001 to 2010 using MODIS eight-day synthetic snow products. The lakes were divided into three groups, among which the lakes in Group C were almost all located in the Inner II. The mean ice cover duration of lakes in Group C was 126 days with a shortening trend of 1.6 day/year, while the mean ice cover duration of lakes in the Inner II in this study is 128 days from 2001 to 2017, and the mean change rate of 21 lakes is −0.89 day/year. The two mean ice cover durations are similar, the change trends are consistent, and the lower rate in this study may be caused by gentler change in recent years. Yao et al. (2016) used MODIS and Landsat data to study lake ice phenology in the Hoh Xil region from 2000 to 2011. Their mean ice cover duration was 196 days with a mean change rate of −1.91 day/year. The Hoh Xil region is in central Inner I, and the lakes analyzed in their study include Dogaicoring Qangco, Taiyang Lake, Hoh Xil Lake, Lexiewudan Co, and Margai Caka. This is the region where lake ice phenology has changed drastically in recent years within the TP (Figures 6 and 7). Consistent with the results of this study, Dogaicoring Qangco and Lexiewudan Co are the rare lakes in this region with advancing freezeup dates and delayed breakup dates, and the reason for these changes will be discussed in the following section. However, in this study, the freezeup start and breakup end dates of Taiyang Lake have been delayed over 17 years, which is different from an advancing breakup end date in Yao et al. (2016). From 2000 to 2011, the breakup end date of Taiyang Lake did show an advancing trend with a rate of 1.51 day/year. However, since 2010, the breakup end date has been delayed annually with a change rate of 3.23 day/year until 2017, which results in an overall delayed trend from 2001 to 2017. Furthermore, many studies have shown that some large lakes on the TP such as Qinghai Lake and Nam Co show a significant delayed trend in freezeup dates and an advancing trend in breakup dates, and the ice cover durations have shortened in recent years (Cai et al., 2017; Che et al., 2009; Ke et al., 2013), which is consistent with the results of this study.

5.2. Influencing Factors on Lake Ice Phenology

5.2.1. Climatic Factors

The low spatial resolution of the reanalysis data makes it difficult to ensure that the inverse distance weighted-interpolated air temperature/wind speed can represent the actual local situation for each single lake. However, the large-scale spatial distribution of meteorological factors and the change rates of the lakes over 17 years on the TP can be obtained from the data. In addition, available lake surface water temperature (LSWT) data for 57 lakes (except for Youbucuo Lake in the Inner II) from 2002 to 2015 derived from MODIS land surface temperature products by Wan et al. (2017) are used.

Compared to the Inner II, the Inner I has a lower mean annual air temperature, LSWT, and wind speed from 2001 to 2017 (Table 4). Under relatively cold conditions with low wind speed, lakes in the Inner I have earlier freezeup dates, later breakup dates, and longer ice cover durations than do lakes in the Inner II. There are

Table 4
Comparison of Climate Conditions Between the Inner I and Inner II From 2001 to 2017 (CR: Change Rates, LSWT: Lake Surface Water Temperature)

	Air Temperature		LSWT (2002–2015)		Wind Speed	
	Mean (°C)	CR (0.01 °C/year)	Mean (°C)	CR (0.01 °C/year)	Mean (m/s)	CR (0.01 m s^{-1} yr^{-1})
Inner I	−6.98	4.30	1.10	−5.26	5.32	1.07
Inner II	−4.94	6.89	5.48	−1.47	5.76	2.31

significant correlations between the ice phenology parameters and climatic factors in the Inner basin, which can pass a two-tailed test with a confidence level of 0.01 (Figure 8). It is probably because the climate factors differ at different lake surroundings (latitude, altitude, etc.) (Guo et al., 2018).

The mean air temperature, LSWT, and wind speed for each of the study lakes are calculated. For every 1 °C increase in air temperature or LSWT or 1-m/s increase in wind speed, the ice cover duration is shortened by 13.75, 18.87, and 29.81 days, respectively (Table 5). LSWT has the highest correlation with lake ice phenology among the three climatic factors (Figure 8 and Table 5; Bussieres et al., 2002). In addition, climate variability and changes have greater effects on lake breakup dates than freezeup dates (Figure 8 and Table 5; Palecki & Barry, 1986).

The energy available for water freezeup in a lake is affected by the heat exchange with the atmosphere, heat stored in the water body, and inflows of water (Williams, 1965). The heat exchange with the atmosphere is mainly determined by climatic factors such as air/water temperature, wind, and solar radiation, while heat storage in a lake is determined additionally by lake morphometry (Brown & Duguay, 2010; Williams, 1965), which will be discussed in the next section. The ice breakup is affected by heat gain from the atmosphere, solar radiation, snow and ice conditions, wind and currents, and inflows (Williams, 1965). Air and water temperature directly drives the lake heat balance and thus plays the main role in the ice cover regime (Kouraev et al., 2007), but the influence of wind is more complex. On the one hand, wind will bring cold or warm currents,

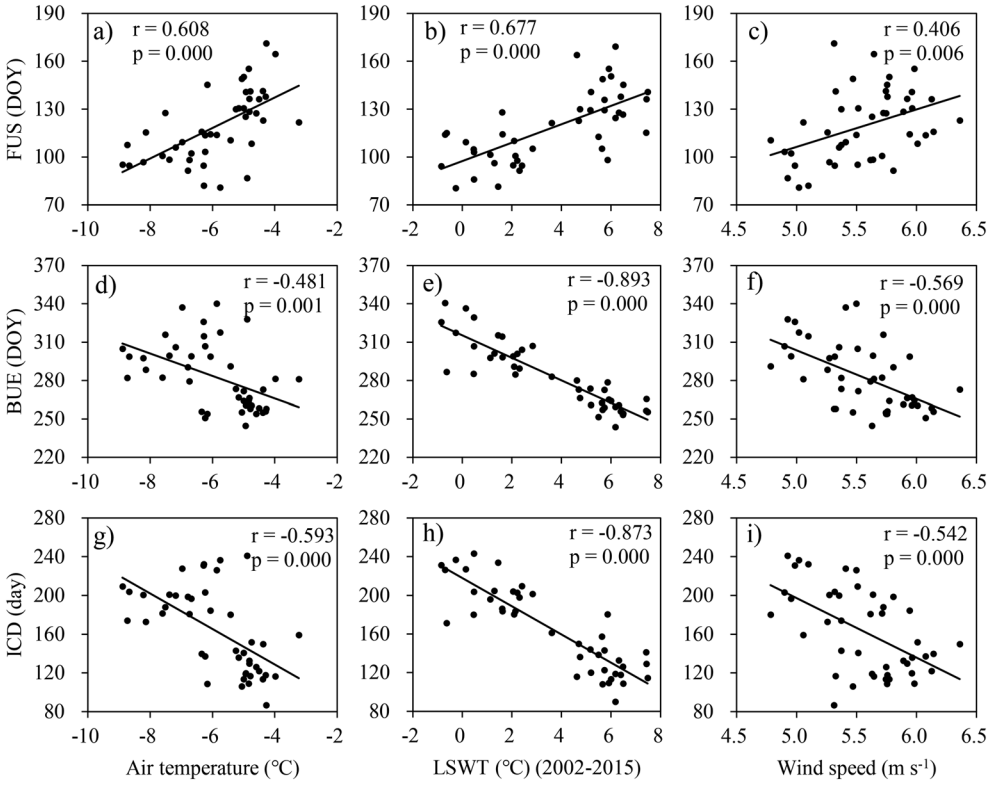

Figure 8. Correlations between mean air temperature, lake surface water temperature (LSWT), wind speed, and mean lake ice phenology parameters in the inner basin from 2001 to 2017. FUS: freezeup start, BUE: breakup end, and ICD: ice cover duration.

Table 5
The Number of Lakes Whose Ice Phenology Has a Significant Correlation ($p < 0.05$) With Climatic Factors, and the Mean Change Rates (FUS: Freezeup Start, BUE: Breakup End, ICD: Ice Cover Duration, and LSWT: Lake Surface Water Temperature)

	Air Temperature (day/°C)	LSWT (day/°C)	Wind Speed (day m^{-1} s)
FUS	7, 8.53	9, 2.55	7, 13.89
BUE	10, −11.11	30, −14.56	11, −26.83
ICD	17, −13.75	23, −18.87	16, −29.81

which affect the water surface temperature, and on the other hand, the dynamic effects of wind could break the thin ice (Brown & Duguay, 2010; Kouraev et al., 2007). However, without detailed field observations, it is difficult to discuss the detailed effects of these climatic factors on lake ice phenology on the TP lakes.

5.2.2. Lake Location, Physico-Chemical Conditions, and Other Factors

To control the differences in climate conditions, the correlations between lake ice phenology and lake altitude, area, and mineralization are calculated separately for the Inner I and Inner II. Some of these lakes have no historical records of mineralization; thus, only the salt lakes with mineralization data are used (Table 6).

There is a significant positive correlation between the altitudes and breakup end dates of the lakes in the Inner basin. The higher the altitude is, the later the breakup end date is and the longer the ice cover duration is. There is an obvious autocorrelation between the altitude and climatic conditions that together affect the breakup time of the lakes, while the freezeup time is mainly affected by the physical and chemical characteristics of the lakes (Adrian et al., 2009; Yao et al., 2016).

Lakes with larger areas have more water-storage capacity and a stronger dynamic effect, resulting in a longer freezeup duration (Yao et al., 2016). Furthermore, wind can break up the initial ice cover more easily (Brown & Duguay, 2010; Kouraev et al., 2007). Lakes with long freezeup durations in the Inner basin such as Qinghai Lake, Selin Co, and Ngangla Ringco are all lakes with areas larger than 500 km^2 (Table A1). In theory, lakes with higher mineralizations should have a lower ice point, as well as a later freezeup date, earlier breakup date, and shorter ice cover duration (Yao et al., 2016). Lakes, such as Selin Co, Nam Co, and Tu Co, with large areas but low mineralization may affect the results of the correlation analysis (Table 6). In this case, lake size has a greater impact on the ice phenology than does the mineralization. At the same time, currently available mineralization records are from the 1970s to 1990s (Wang & Dou, 1998). In the context of climate change, the mineralization of lakes on the TP may have changed greatly over the past several decades. For example, the reduction of lake water volume may lead to increase in mineralization and the expansion of lake area may lead to desalination.

Lexiewudan Co, which has the highest change rate of ice phonology over the 17 years, had a mineralization of 135.50 g/L in 1990 (Wang & Dou, 1998) and dropped to 89.47 g/L in 2010 (He et al., 2015). The lake came through an obvious process of desalination. Apart from this, the lake is recharged with ice-snowmelt water and large amounts of spring water (Wang & Dou, 1998). The special recharge form may also be one of the reasons that caused the large change in ice phenology. In addition, Dogaicoring Qangco may have similar reasons for the large changes in recent years, as the lake is nearby Lexiewudan Co and has similar conditions as Lexiewudan Co.

Shallow lakes require less heat to freezeup and have earlier freezeup dates (Kropáček et al., 2013; Yao et al., 2016). The physical characteristics determine the thermodynamics of a lake and sometimes have

Table 6
Correlations Between Ice Phenology and the Physical Attributes of the Lakes in the Inner I and Inner II (FUS: Freezeup Start, BUE: Breakup End, and ICD: Ice Cover Duration)

	Inner I			Inner II		
	Altitude	Area	Mineralization[a]	Altitude	Area	Mineralization[b]
FUS	0.24	0.44	−0.04	−0.03	0.48*	−0.17
BUE	0.52*	−0.03	−0.28	0.65**	0.18	−0.03
ICD	0.28	−0.26	−0.24	0.34	−0.32	0.15

[a]Calculated from 11 salt lakes. [b]Calculated from 19 salt lakes, and mineralization data are from Wang and Dou (1998). *Statistical significance at the 0.05 level. **Statistical significance at the 0.01 level.

more of an impact on the ice phenology than do the chemical conditions. For example, the weather conditions of Gahai and Qinghai Lake are similar, and the freezeup dates are nearly on the same day. As one of the remaining sublakes of Qinghai Lake, Gahai has no surface inflow and a smaller area (Gahai: 44.68 km^2, Qinghai Lake: 4,254.90 km^2, Wan et al., 2014) as well as a shallower depth (Gahai: 8.0–9.5 m, Qinghai Lake: average of 17.9 m; Wang & Dou, 1998). Although Gahai has a higher mineralization of 31.73 g/L than that of Qinghai Lake (13.84 g/L; Wang & Dou, 1998), the mean freezeup start date is 15 days earlier than that of Qinghai Lake.

6. Conclusions

Approximately two thirds of the cloud cover from the MODIS daily snow cover products can be eliminated by gap-filling approach combining Terra and Aqua data and using the pixels within two days before and after the cloud-covered pixel. The water cover classification from cloud-removed MODIS data agrees well with the Landsat data (28 scenes, MAE = 4.58%) for two validated lakes (Nam Co and Selin Co) during the freezeup and breakup periods. On this basis, the freezeup start and breakup end dates of the 58 lakes on the TP from 2001 to 2017 are extracted. The freezeup end and breakup start dates of 18 lakes were simultaneously extracted, and the lake ice durations (including freezeup duration, complete freezing duration, breakup duration, and ice cover duration) are calculated based on freezeup/breakup dates. Compared to freezeup dates (MAEs range from 2.92 to 7.25 days), the breakup dates (MAEs range from 1.75 to 3.25 days) have a better consistent with different passive microwave data sets derived from AMSR-E/2 and SSM/I.

From late October to mid-January of the following year, the lakes on the TP begin to freeze one after another (mainly from northern part to southern part). Over 17 years, the freezeup start dates of 47 lakes have been delayed at a mean rate of 0.55 day/year, and the other 11 lakes have advancing freezeup start date at a mean change rate of 0.44 day/year. From late March to early July, the lakes gradually end their ice cover periods (mainly from southern part to northern part). Over 17 years, the lakes whose breakup end dates have been delayed and advanced account for 50% each, with mean change rates of 0.69 and 0.39 day/year, respectively. The mean ice cover duration of 58 lakes is 157.78 days, of which the shortest is 86.59 days, and the longest is 240.94 days. From 2001 to 2017, there are 18 lakes with ice cover durations that extended at a mean change rate of 1.11 day/year, and 40 lakes shortened their ice cover durations at a mean change rate of 0.80 day/year. Furthermore, the freezeup and breakup processes of 18 lakes are extracted; the mean freezeup duration is 9.81 days, the mean breakup duration is 13.01 days, and the mean complete freezing duration is 121.12 days. Most lakes have shorter freezeup durations than breakup durations, and the freezeup and breakup rates of most lakes have increased over the 17 years.

The ice phenology is influenced by climatic conditions, geographical location, and the physico-chemical characteristics of the lake. Lakes in the region with a lower altitude, higher air/water temperature, and higher wind speed are inclined to have later freezeup and earlier breakup dates, as well as shorter ice cover durations. The physico-chemical characteristics of the lakes mainly affect the freezeup dates; deeper lakes with larger areas and higher mineralization tend to have later freezeup dates. Sometimes lake physical conditions may have a greater impact on ice phenology than do the chemical conditions.

The lack of historical observational data makes it difficult to study lake ice phenology on the TP without using remote sensing data. The quality of MODIS daily snow cover products limits the number of lakes that can be studied, and the low spatial resolution of reanalysis data makes it difficult to represent the actual meteorological conditions of each lake. It is also difficult to ensure the reliability of historical lake physico-chemical data that were collected several decades ago. With the improvement of data and methods, lake ice phenology on the TP and its influencing factors can hopefully be further analyzed in the future. In addition, further research is required on the comparisons of lake ice phenology characteristics derived from different sources of remote sensing data and different retrieval methods, as well as in different climatic regions.

Appendix A

Mean values and change rates of lake ice phenology are shown in Table A1, including the freezeup start date, breakup end date, and ice cover duration for 58 lakes, as well as eight parameters (freezeup start date, freezeup end date, breakup start date, breakup end date, freezeup duration, breakup duration, complete freezing

Journal of Geophysical Research: Atmospheres
10.1029/2018JD028993

Table A1

Lake Ice Phenology Statistics and the Change Rates (CR; day/year) and Lake Characteristics for 58 Lakes From 2001 to 2017 (FUS: Freezeup Start, FUE: Freezeup End, BUS: Breakup Start, BUE: Breakup End, FUD: Freezeup Duration, BUD: Breakup Duration, CFD: Complete Freezing Duration, and ICD: Ice Cover Duration)

No.	Lake	Area (km^2)[a]	Altitude (m)[b]	Mean FUS	CR	Mean FUE	CR	Mean BUS	CR	Mean BUE	CR	Mean FUD	CR	Mean CFD	CR	Mean BUD	CR	Mean ICD	CR	Spatial Location
1	Bamco	236.16	4560	16 December	0.82*					13 April	0.25							117.88	−0.56	II
2	Bangkog Co	136.34	4527	17 November	1.10*					18 April	−1.63**							151.82	−2.73**	II
3	Burog Co	89.91	5166	18 November	0.88**					4 July	−0.39							227.82	−1.26	I
4	Changhu Lake	49.98	4839	4 November	−0.24					1 June	0.28							209.29	0.52	I
5	Cuoda Rima	84.60	4783	11 November	0.13					26 May	0.42							196.59	0.29	I
6	Cuona Lake	188.54	4585	3 December	0.19					25 March	0.36							112.06	0.16	II
7	Dagze Co	269.07	4465	15 December	0.79**	20 December	0.63*	2 April	0.82	16 April	0.20	5.18	−0.16	103.59	0.19	13.35	−0.63**	122.12	−0.59	II
8	Dawa Co	110.55	4623	9 December	0.85*	14 December	0.71*	12 April	0.07	29 April	0.00	4.94	−0.14	118.65	−0.64*	17.29	−0.07	140.88	−0.85	II
9	Dogaicoring Qangco	313.68	4787	16 November	−1.12					9 May	3.50*							174.24	4.62	I
10	Dong Co	92.47	4394	22 November	0.27	28 November	0.20	1 April	1.10	8 April	1.02	6.18	−0.07	123.65	0.90	7.29	−0.08	137.12	0.75	II
11	Donggei Cuona Lake	230.65	4081	15 December	0.23*					10 May	0.21							145.53	−0.02	III
12	Dung Co	149.60	4551	6 December	0.77**					11 April	−0.35							126.29	−1.12	II
13	Gahai	44.68	3197	3 December	0.38					4 April	0.01							121.29	−0.37	III
14	Garkung Caka	59.33	4909	7 November	−0.04					27 May	0.13							200.82	0.17	I
15	Gemang Co	60.06	4605	15 December	0.35					24 April	0.05							129.76	−0.30	II
16	Gopug Co	59.68	4718	7 November	0.15					7 May	−0.88							181.00	−1.03	II
17	Goren Co	477.98	4649	29 December	0.25					21 April	0.25							113.59	0.00	II
18	Gozha Co	315.51	5080	22 November	0.67**					7 July	0.03							226.12	−0.64	I
19	Gyaring Lake	526.62	4290	16 November	1.02*					18 April	−0.27							153.12	−1.29	III
20	Har Lake	596.39	4076	18 November	0.66**	27 November	0.35	24 May	−0.38	3 June	−0.12	9.06	−0.30	177.35	−0.73*	10.47	0.26	196.88	−0.77*	III
21	Hoh Xil Lake	315.95	4886	3 November	0.47	15 November	0.15	12 June	0.93*	22 June	0.58	11.47	−0.33	209.65	0.79	9.88*	−0.35	231.00	0.11	I
22	Huolunuo'er	259.24	4753	12 November	−0.64					3 June	−0.65							203.35	−0.01	I
23	Keluke Lake	54.00	2814	27 November	0.14					27 March	−0.40							119.35	−0.54	III
24	Kusai Lake	271.08	4475	19 November	0.80**	4 December	0.51*	6 May	0.09	18 May	−0.10	14.65	−0.28	153.71	−0.42	11.94	−0.19	180.29	−0.90*	I
25	Kyebxang Co	170.98	4615	1 December	0.48	9 December	0.42*	17 April	0.51	30 April	−0.01	7.59	−0.06	128.71	0.10	13.65	−0.52	149.94	−0.48	II
26	Lagkor Co	93.39	4467	24 December	0.80**	28 December	0.86**	30 March	−0.27	11 April	0.00	3.94	0.06	92.65	−1.13*	12.00	0.26	108.59	−0.81	II
27	Laxiong Co	60.75	4885	15 November	0.62**					2 June	−0.38							199.88	−1.01	I
28	Lexiewudan Co	247.58	4870	24 November	−1.22**					16 May	4.25**							172.76	5.46**	I
29	Lingguo Co	108.14	5062	6 December	−0.19					12 June	0.63							188.06	0.82	I
30	Longwei Co	52.88	4942	9 November	−0.52					10 May	1.40							181.41	1.93	I
31	Mapam Yumco	409.90	4585	13 January	0.00	22 January	0.04	20 April	0.13	29 April	−0.08	9.60	0.02	87.86	0.09	8.61	0.00	106.06	−0.08	III
32	Margai Caka	145.17	4793	3 November	0.50**					26 May	−0.64							203.82	−1.15*	I
33	Meiriqiecuomari	86.00	4947	31 October	−0.01					18 May	−0.58							198.65	−0.57	I
34	Nam Co	2040.90	4724	12 January	0.51					9 May	−0.21							116.59	−0.72	II
35	Ngangla Ringco	542.89	4716	9 December	0.75*	27 December	0.51*	14 April	0.30	1 May	0.10	18.76	−0.24	107.76	−0.21*	16.65	−0.20	143.18	−0.65	II
36	Ngangze Co	445.48	4685	4 December	1.25**	11 December	1.04	18 March	1.42	2 April	0.42	7.43	−0.15	96.50	0.38	15.18	−0.80	119.12	−0.82	II
37	Ngoring Lake	629.75	4267	1 December	0.25					8 May	−0.02							158.00	−0.27	III
38	Palung Co	144.65	5101	30 November	0.18	8 December	0.31	20 April	−0.34	8 May	−0.20	7.94	0.12	132.47	−0.65	18.65	0.14	159.06	−0.38	II
39	Puma Yumco	294.11	5013	1 January	0.41					1 May	−0.54							120.24	−0.95	III
40	Pung Co	172.11	4529	20 December	0.75**					12 April	−0.29							113.59	−1.05	II
41	Qinghai Lake	4254.90	3194	18 December	0.40	6 January	0.49	23 March	−0.50	4 Apr	−0.07	18.59	0.09	76.82	−0.99**	11.94	0.43	107.35	−0.47	III

Journal of Geophysical Research: Atmospheres

10.1029/2018JD028993

Table A1 *(continued)*

No.	Lake	Area (km^2)[a]	Altitude (m)[b]	Mean FUS	CR	Mean FUE	CR	Mean BUS	CR	Mean BUE	CR	Mean FUD	CR	Mean CFD	CR	Mean BUD	CR	Mean ICD	CR	Spatial Location
42	Rola Co	82.52	4815	5 November	−0.36					25 May	1.24							200.59	1.60	I
43	Selin Co	2129.02	4539	19 December	0.71*	5 January	0.55	4 April	0.15	18 April	−0.56	16.29	−0.17	89.71	−0.39	13.76	−0.71**	119.76	−1.27*	II
44	Sugan Lake	101.40	2793	18 November	0.10	29 November	0.51	28 March	0.33	10 April	0.13	10.59	0.41	119.12	−0.19*	13.59	−0.20	143.29	0.02	III
45	Taiyang Lake	101.82	4881	22 November	0.46*					18 June	0.56							207.65	0.10	III
46	Taro Co	486.62	4567	19 January	0.16					15 April	−0.40							86.59	−0.56	II
47	Telashi Lake	63.15	4805	4 November	0.19					27 May	0.86							203.94	0.67	III
48	Tu Co	428.00	4929	23 November	−0.52	1 December	−0.93*	13 May	2.11*	26 May	1.70**	8.47	−0.41	163.24	3.04	12.65	−0.41	184.35	2.22**	I
49	Tuosu Lake	137.76	2805	24 December	0.17					25 March	−0.06							90.24	−0.23	III
50	Urru Co	362.52	4554	3 January	0.01					22 April	0.48							109.00	0.47	II
51	Xuejing Lake	72.73	4807	22 October	0.64**					11 June	−0.26							232.47	−0.91	I
52	Xuemei Lake	41.33	4873	26 October	0.30					24 June	0.34							240.94	0.04	I
53	Yaggain Co	97.41	4534	7 December	1.48**					19 April	0.10							132.82	−1.38**	II
54	Youbucuo Lake	63.19	4640	20 December	0.56*					15 April	−0.14							116.71	−0.70	II
55	Yuye Lake	126.36	4856	20 October	0.73**					14 June	−1.08							236.71	−1.81*	I
56	Zhari Namco	990.26	4612	27 December	0.64*	7 January	0.48	31 March	0.74	13 April	0.63	10.41	−0.17	83.29	0.26*	12.41	−0.11	106.12	−0.01	II
57	Zhaxi Co	47.47	4416	24 November	0.70**					13 April	−0.89**							139.71	−1.59**	II
58	Zige Tangco	225.55	4568	9 December	1.01**	15 December	0.94**	9 Apr	−0.17	24 April	−0.12	5.53	−0.07	115.47	−1.11*	14.88	0.05	135.88	−1.13*	II

[a]Wan et al. (2014). [b]The altitudes of lakes are derived from Shuttle Radar Topography Mission (SRTM) digital elevation model (DEM) data (http://srtm.csi.cgiar.org/SELECTION/inputCoord.asp).
*Statistical significance at the 0.05 level (Mann-Kendall test). **Statistical significance at the 0.01 level (Mann-Kendall test).

Table A2
Lake Ice Phenology Statistics From 2001 to 2017 (FUS: Freezeup Start, FUE: Freezeup End, BUS: Breakup Start, BUE: Breakup End, FUD: Freezeup Duration, BUD: Breakup Duration, CFD: Complete Freezing Duration, and ICD: Ice Cover Duration)

		Mean[a]	Minimum	Maximum	Max-Min	Median	Standard Deviation
Mean date/days	FUS[c]	30 November	20 Oct (Yuye Lake)	19 Jan (Taro Co)	90.47	29 November	21.57
	FUE[b]	16 December	15 Nov (Hoh Xil Lake)	22 Jan (Mapam Yumco)	68.48	13 December	17.81
	BUS[b]	16 April	18 Mar (Ngangze Co)	12 Jun (Hoh Xil Lake)	86.60	10 April	22.78
	BUE[c]	6 May	25 Mar (Tuosu Lake)	7 Jul (Gozha Co)	104.00	1 May	26.62
	FUD[b]	9.81	3.94 (Lagkor Co)	18.76 (Ngangla Ringco)	14.82	8.76	4.56
	BUD[b]	13.01	7.29 (Dong Co)	18.65 (Palung Co)	11.35	13.00	2.92
	CFD[b]	121.12	76.82 (Qinghai Lake)	209.65 (Hoh Xil Lake)	132.82	117.06	35.53
	ICD[c]	157.78	86.59 (Taro Co)	240.94 (Xuemei Lake)	154.35	147.74	42.99
Change rate (day/year)	FUS	0.53	−1.22 (Lexiewudan Co)	1.48 (Yaggain Co)	2.70		0.52
	FUE	0.54	−0.93 (Tu Co)	1.04 (Ngangze Co)	1.97		0.43
	BUS	0.58	−0.50 (Qinghai Lake)	2.11 (Tu Co)	2.61		0.69
	BUE	0.54	−1.63 (Bangkog Co)	4.25 (Lexiewudan Co)	5.88		0.92
	FUD	0.18	−0.41 (Tu Co)	0.41 (Sugan Lake)	0.82		0.20
	BUD	0.30	−0.80 (Ngangze Co)	0.43 (Qinghai Lake)	1.24		0.35
	CFD	0.68	−1.13 (Lagkor Co)	3.04 (Tu Co)	4.17		0.97
	ICD	0.90	−2.73 (Bangkog Co)	5.46 (Lexiewudan Co)	8.20		1.32

[a]The mean change rates of lake ice phenology are mean absolute values. [b]Calculated from 18 lakes. [c]Calculated from 58 lakes.

duration, and ice cover duration) for 18 lakes. Trend significances of dates and durations changes are evaluated by Mann-Kendall test, and the significances are labeled in Table A1. Lakes on the TP freeze up in succession from October to January of the following year and break up from March to July. From 2001 to 2017, the number of freezeup dates with a significant change trend ($p < 0.05$) is larger than that of breakup dates (27 for freezeup start and 8 for freezeup end compared to 2 for breakup start and 5 for breakup end date). In addition, lake area, altitude, and belonged subareas (refer to Figure 1) are also provided in Table A1. There are 20, 24, and 14 lakes in inner I, inner II, and other III, respectively.

Calculated statistics of lake ice phenology are shown in Table A2, including mean values, extreme values, extreme difference, median, and standard deviation of all the lakes. The lakes where the extreme values appear are also attached. The mean ice cover duration of lakes on the TP is 157.78 days, and the mean change rate from 2001 to 2017 is 0.90 day/year. The lakes with the shortest and longest ice cover duration are Taro Co (86.59 days) and Xuemei Lake (240.94 days), respectively. The lake with the highest shortening rate of ice cover duration during 17 years is Bangkog Co (−2.73 day/year), and the lake with the highest extending rate is Lexiewudan Co (5.46 day/year).

Acknowledgments
This work is supported financially by National Natural Science Foundation of China (41830105) and also funded by the International Scholar Exchange Fellowship (ISEF) program at KFAS (Korean Foundation of Advanced Studies). The MODIS snow data used in this study are obtained from the National Snow and Ice Data Center (http://nsidc.org). The Landsat data used are obtained from the Google Earth Engine platform (https://earthengine.google.com/). The Reanalysis data are from the National Oceanic and Atmospheric Administration (https://www.esrl.noaa.gov/). We would thank the two anonymous reviewers and the editors for their valuable comments and suggestions to greatly improve the paper.

References

Adrian, R., O'Reilly, C. M., Zagarese, H., Baines, S. B., Hessen, D. O., Keller, W., et al. (2009). Lakes as sentinels of climate change. *Limnology and Oceanography*, *54*(6part2), 2283–2297. https://doi.org/10.4319/lo.2009.54.6_part_2.2283

Brown, L. C., & Duguay, C. R. (2010). The response and role of ice cover in lake-climate interactions. *Progress in Physical Geography*, *34*(5), 671–704. https://doi.org/10.1177/0309133310375653

Bussieres, N., Verseghy, D., & MacPherson, J. I. (2002). The evolution of AVHRR-derived water temperatures over boreal lakes. *Remote Sensing of Environment*, *80*(3), 373–384. https://doi.org/10.1016/S0034-4257(01)00317-0

Cai, Y., Ke, C. Q., & Duan, Z. (2017). Monitoring ice variations in Qinghai Lake from 1979 to 2016 using passive microwave remote sensing data. *Science of the Total Environment*, *607–608*, 120–131. https://doi.org/10.1016/j.scitotenv.2017.07.027

Chaouch, N., Temimi, M., Romanov, P., Cabrera, R., McKillop, G., & Khanbilvardi, R. (2014). An automated algorithm for river ice monitoring over the Susquehanna River using the MODIS data. *Hydrological Processes*, *28*(1), 62–73. https://doi.org/10.1002/hyp.9548

Che, T., Li, X., & Jin, R. (2009). Monitoring the frozen duration of Qinghai Lake using satellite passive microwave remote sensing low frequency data (in Chinese). *Chinese Science Bulletin*, *54*(13), 2294–2299. https://doi.org/10.1007/s11434-009-0044-3

Dörnhöfer, K., & Oppelt, N. (2016). Remote sensing for lake research and monitoring-recent advances. *Ecological Indicators*, *64*, 105–122. https://doi.org/10.1016/j.ecolind.2015.12.009

Du, J. Y., Kimball, J. S., Duguay, C., Kin, Y., & Watts, J. D. (2017). Satellite microwave assessment of northern hemisphere lake ice phenology from 2002 to 2015. *The Cryosphere*, *11*, 1–26. https://doi.org/10.5194/tc-2016-199

Duguay, C. R., Bernier, M., Gauthier, Y., & Kouraev, A. (2015). Remote sensing of lake and river ice. In M. Tedesco (Ed.), *Remote Sensing of the Cryosphere*, (pp. 273–306). Oxford, UK: Wiley-Blackwell. https://doi.org/10.1002/9781118368909.ch12

Duguay, C. R., & Lafleur, P. M. (2003). Estimating depth and ice thickness of shallow subarctic lakes using spaceborne optical and SAR data. *International Journal of Remote Sensing*, *24*(3), 475–489. https://doi.org/10.1080/01431160304992

Duguay, C. R., Pultz, T. J., Lafleur, P. M., & Drai, D. (2002). RADARSAT backscatter characteristics of ice growing on shallow sub-arctic lakes, Churchill, Manitoba, Canada. *Hydrological Processes*, *16*(8), 1631–1644. https://doi.org/10.1002/hyp.1026

Gafurov, A., & Bárdossy, A. (2009). Cloud removal methodology from MODIS snow cover product. *Hydrology and Earth System Sciences*, *13*(7), 1361–1373. https://doi.org/10.5194/hess-13-1361-2009

Gao, Y., Xie, H. J., Lu, N., Yao, T. D., & Liang, T. G. (2010). Toward advanced daily cloud-free snow cover and snow water equivalent products from Terra–Aqua MODIS and aqua AMSR-E measurements. *Journal of Hydrology*, *385*(1–4), 23–35. https://doi.org/10.1016/j.jhydrol.2010.01.022

Gao, Y., Xie, H. J., Yao, T. D., & Xue, C. S. (2010). Integrated assessment on multi-temporal and multi-sensor combinations for reducing cloud obscuration of MODIS snow cover products of the Pacific Northwest USA. *Remote Sensing of Environment*, *114*(8), 1662–1675. https://doi.org/10.1016/j.rse.2010.02.017

Geldsetzer, T., Sanden, J. V. D., & Brisco, B. (2010). Monitoring lake ice during spring melt using RADARSAT-2 SAR. *Canadian Journal of Remote Sensing*, *36*(sup2), S391–S400. https://doi.org/10.5589/m11-001

Guo, L. N., Wu, Y. H., Zheng, H. X., Zhang, B., Li, J. S., Zhang, F. F., & Shen, Q. (2018). Uncertainty and variation of remotely sensed lake ice phenology across the Tibetan Plateau. *Remote Sensing*, *10*(10), 1534. https://doi.org/10.3390/rs10101534

Hall, D. K., & Riggs, G. A. (2007). Accuracy assessment of the MODIS snow products. *Hydrological Processes*, *21*(12), 1534–1547. https://doi.org/10.1002/hyp.6715

Hall, D. K., Riggs, G. A. & Salomonson, V. V. (2001). Algorithm Theoretical Basis Document (ATBD) for the MODIS Snow and Sea Ice-Mapping Algorithms. https://modis-snow-ice.gsfc.nasa.gov/?c=atbd&t=atbd

He, L., Han, F. Q., Han, W. X., Yan, J. P., Li, B. K., Han, Y. Z., et al. (2015). Hydrochemical characteristics of Lexiewudan Lake in Hoh Xil, Qinghai (in Chinese). *Journal of Salt Lake Research*, *23*(2), 28–33.

Howell, S. E. L., Brown, L. C., Kang, K. -K., & Duguay, C. R. (2009). Variability in ice phenology on Great Bear Lake and Great Slave Lake, Northwest Territories, Canada, from SeaWinds/QuikSCAT: 2000–2006. *Remote Sensing of Environment*, *113*(4), 816–834. https://doi.org/10.1016/j.rse.2008.12.007

Huang, H., Liang, T., Zhang, X., & Guo, Z. (2011). Validation of MODIS snow cover products using Landsat and ground measurements during the 2001–2005 snow seasons over northern Xinjiang, China. *International Journal of Remote Sensing*, *32*(1), 133–152. https://doi.org/10.1080/01431160903439924

Jeffries, M. O., Morris, K., Weeks, W. F., & Wakabayashi, H. (1994). Structural and stratigraphic features and ERS 1 synthetic aperture radar backscatter characteristics of ice growing on shallow lakes in NW Alaska, winter 1991–1992. *Journal of Geophysical Research*, *99*, 22,459–22,471. https://doi.org/10.1029/94JC01479

Kang, S. C., Xu, Y. W., You, Q. L., Flügel, W. -A., Pepin, N., & Yao, T. D. (2010). Review of climate and cryospheric change in the Tibetan Plateau. *Environmental Research Letters*, *5*(1), 015101. https://doi.org/10.1088/1748-9326/5/1/015101

Ke, C. Q., Tao, A. Q., & Jin, X. (2013). Variability in the ice phenology of Nam Co Lake in central Tibet from scanning multichannel microwave radiometer and special sensor microwave/imager: 1978 to 2013. *Journal of Applied Remote Sensing*, *7*(1), 073477. https://doi.org/10.1117/1.JRS.7.073477

Kendall, M. G. (1975). *Rank Correlation Methods*. London: Charles Griffin.

Kouraev, A. V., Semovski, S. V., Shimaraev, M. N., Mognard, N. M., Legrésy, B., & Rémy, F. (2007). The ice regime of Lake Baikal from historical and satellite data: Relationship to air temperature, dynamical, and other factors. *Limnology and Oceanography*, *52*(3), 1268–1286. https://doi.org/10.4319/lo.2007.52.3.1268

Kropáček, J., Maussion, F., Chen, F., Hoerz, S., & Hochschild, V. (2013). Analysis of ice phenology of lakes on the Tibetan Plateau from MODIS data. *The Cryosphere*, *7*(1), 287–301. https://doi.org/10.5194/tc-7-287-2013

Latifovic, R., & Pouliot, D. (2007). Analysis of climate change impacts on lake ice phenology in Canada using the historical satellite data record. *Remote Sensing of Environment*, *106*(4), 492–507. https://doi.org/10.1016/j.rse.2006.09.015

Liang, T. G., Zhang, X. T., Xie, H. J., Wu, C. X., Feng, Q. S., Huang, X. D., & Chen, Q. G. (2008). Toward improved daily snow cover mapping with advanced combination of MODIS and AMSR-E measurements. *Remote Sensing of Environment*, *112*(10), 3750–3761. https://doi.org/10.1016/j.rse.2008.05.010

Liu, X. D., & Chen, B. D. (2000). Climatic warming in the Tibetan Plateau during recent decades. *International Journal of Climatology*, *20*(14), 1729–1742. https://doi.org/10.1002/1097-0088(20001130)20:14<1729::AID-JOC556>3.0.CO;2-Y

López-Burgos, V., Gupta, H. V., & Clark, M. (2013). Reducing cloud obscuration of MODIS snow cover area products by combining spatio-temporal techniques with a probability of snow approach. *Hydrology and Earth System Sciences*, *17*(5), 1809–1823. https://doi.org/10.5194/hess-17-1809-2013

Mann, H. B. (1945). Non-parametric tests against trend. *Econometrica*, *13*(3), 245–259. https://doi.org/10.2307/1907187

Maurer, E. P., Rhoads, J. D., Dubayah, R. O., & Lettenmaier, D. P. (2003). Evaluation of the snow-covered area data product from MODIS. *Hydrological Processes*, *17*(1), 59–71. https://doi.org/10.1002/hyp.1193

Morris, K., Jeffries, M. O., & Weeks, W. F. (1995). Ice processes and growth history on Arctic and sub-Arctic lakes using ERS-1 SAR data. *Polar Record*, *31*(177), 115–128. https://doi.org/10.1017/S0032247400013619

Palecki, M. A., & Barry, R. G. (1986). Freeze-up and break-up of lakes as an index of temperature changes during the transition seasons: A case study for Finland. *Journal of Climate and Applied Climatology*, *25*(7), 893–902. https://doi.org/10.1175/1520-0450(1986)025<0893:FUABUO>2.0.CO;2

Parajka, J., & Blöschl, G. (2008). The value of MODIS snow cover data in validating and calibrating conceptual hydrologic models. *Journal of Hydrology*, *358*(3–4), 240–258. https://doi.org/10.1016/j.jhydrol.2008.06.006

Paudel, K. P., & Andersen, P. (2011). Monitoring snow cover variability in an agropastoral area in the trans Himalayan region of Nepal using MODIS data with improved cloud removal methodology. *Remote Sensing of Environment*, *115*(5), 1234–1246. https://doi.org/10.1016/j.rse.2011.01.006

Qiu, J. (2008). The third pole. *Nature*, *454*(7203), 393–396. https://doi.org/10.1038/454393a

Reed, B., Buddle, M., Spencer, P., & Miller, A. E. (2009). Integration of MODIS-derived metrics to assess interannual variability in snowpack, lake ice, and NDVI in Southwest Alaska. *Remote Sensing of Environment*, *113*(7), 1443–1452. https://doi.org/10.1016/j.rse.2008.07.020

Rouse, W. R., Oswald, C. J., Binyamin, J., Spence, C., Schertzer, W. M., Blanken, P. D., Bussières, N., et al. (2005). The role of Northern Lakes in a regional energy balance. *Journal of Hydrometeorology*, *6*(3), 291–305. https://doi.org/10.1175/JHM421.1

Sorman, A. U., Akyurek, Z., Sensoy, A., Sorman, A. A., & Tekeli, A. E. (2007). Commentary on comparison of MODIS snow cover and albedo products with ground observations over the mountainous terrain of Turkey. *Hydrology and Earth System Sciences*, *11*(4), 1353–1360. https://doi.org/10.5194/hess-11-1353-2007

Wan, W., Li, H., Xie, H. J., Hong, Y., Long, D., Zhao, L. M., et al. (2017). A comprehensive data set of lake surface water temperature over the Tibetan Plateau derived from MODIS LST products 2001–2015. *Scientific Data*, *4*. https://doi.org/10.1038/sdata.2017.95

Wan, W., Xiao, P. F., Feng, X. Z., Li, H., Ma, R. H., Duan, H. T., & Zhao, L. M. (2014). Monitoring lake changes of Qinghai-Tibetan Plateau over the past 30 years using satellite remote sensing data. *Chinese Science Bulletin*, *59*(10), 1021–1035. https://doi.org/10.1007/s11434-014-0128-6

Wang, S. M., & Dou, H. S. (1998). *Records of Chinese Lakes (in Chinese)*. Beijing, CHN: Science Press.

Weber, H., Riffler, M., Nõges, T., & Wunderle, S. (2016). Lake ice phenology from AVHRR data for European lakes: An automated two-step extraction method. *Remote Sensing of Environment*, *174*, 329–340. https://doi.org/10.1016/j.rse.2015.12.014

Wei, Q. F., & Ye, Q. H. (2010). Review of lake ice monitoring by remote sensing (in Chinese). *Progress in Geography*, *29*(7), 803–810.

Williams, G. P. (1965). Correlating freeze-up and break-up with weather conditions. *Canadian Geotechnical Journal*, *2*(4), 313–326. https://doi.org/10.1139/t65-047

Yao, X. J., Li, L., Zhao, J., Sun, M. P., Li, J., Gong, P., & An, L. N. (2016). Spatial-temporal variations of lake ice phenology in the Hoh Xil region from 2000 to 2011. *Journal of Geographical Sciences*, *26*(1), 70–82. https://doi.org/10.1007/s11442-016-1255-6

Yu, J. Y., Zhang, G. Q., Yao, T. D., Xie, H. J., Zhang, H. B., Ke, C. Q., & Yao, R. Z. (2016). Developing daily cloud-free snow composite products from MODIS Terra–Aqua and IMS for the Tibetan Plateau. *IEEE Transactions on Geoscience and Remote Sensing*, *54*(4), 2171–2180. https://doi.org/10.1109/TGRS.2015.2496950

Zhang, G. Q., Yao, T. D., Xie, H. J., Kang, S. C., & Lei, Y. B. (2013). Increased mass over the Tibetan Plateau: From lakes or glaciers? *Geophysical Research Letters*, *40*, 2125–2130. https://doi.org/10.1002/grl.50462

Zhang, G. Q., Yao, T. D., Xie, H. J., Qin, J., Ye, Q. H., Dai, Y. F., & Guo, R. F. (2014). Estimating surface temperature changes of lakes in the Tibetan Plateau using MODIS LST data. *Journal of Geophysical Research: Atmospheres*, *119*, 8552–8567. https://doi.org/10.1002/2014JD021615

Zhang, G. Q., Yao, T. D., Xie, H. J., Zhang, K. X., & Zhu, F. J. (2014). Lakes' state and abundance across the Tibetan Plateau. *Chinese Science Bulletin*, *59*(24), 3010–3021. https://doi.org/10.1007/s11434-014-0258-x